AGU PUBLICATIONS

Geochemistry, Geophysics, Geosystems

RESEARCH ARTICLE
10.1002/2016GC006457

The Fina Nagu volcanic complex: Unusual submarine arc volcanism in the rapidly deforming southern Mariana margin

Maryjo Brounce[1,2], Katherine A. Kelley[3], Robert Stern[4], Fernando Martinez[5], and Elizabeth Cottrell[6]

[1]Division of Geological and Planetary Sciences, California Institute of Technology, Pasadena, California, USA, [2]Now at: Department of Earth Science, University of California Riverside, Riverside, California, USA, [3]Graduate School of Oceanography, University of Rhode Island, Narragansett, Rhode Island, USA, [4]Geosciences Department, University of Texas at Dallas, Richardson, Texas, USA, [5]Hawai'i Institute of Geophysics and Planetology, University of Hawai'i at Manoa, Honolulu, Hawaii, USA, [6]Department of Mineral Sciences, National Museum of Natural History, Smithsonian Institution, Washington, DC, USA

Abstract In the Mariana convergent margin, large arc volcanoes disappear south of Guam even though the Pacific plate continues to subduct and instead, small cones scatter on the seafloor. These small cones could form either due to decompression melting accompanying back-arc extension or flux melting, as expected for arc volcanoes, or as a result of both processes. Here, we report the major, trace, and volatile element compositions, as well as the oxidation state of Fe, in recently dredged, fresh pillow lavas from the Fina Nagu volcanic chain, an unusual alignment of small, closely spaced submarine calderas and cones southwest of Guam. We show that Fina Nagu magmas are the consequence of mantle melting due to infiltrating aqueous fluids and sediment melts sourced from the subducting Pacific plate into a depleted mantle wedge, similar in extent of melting to accepted models for arc melts. Fina Nagu magmas are not as oxidized as magmas elsewhere along the Mariana arc, suggesting that the subduction component responsible for producing arc magmas is either different or not present in the zone of melt generation for Fina Nagu, and that amphibole or serpentine mineral destabilization reactions are key in producing oxidized arc magmas. Individual Fina Nagu volcanic structures are smaller in volume than Mariana arc volcanoes, although the estimated cumulative volume of the volcanic chain is similar to nearby submarine arc volcanoes. We conclude that melt generation under the Fina Nagu chain occurs by similar mechanisms as under Mariana arc volcanoes, but that complex lithospheric deformation in the region distributes the melts among several small edifices that get younger to the northeast.

Key Points:
- The Fina Nagu volcanic chain is an unusual chain of small volcanoes marking the southern extension of the Mariana arc
- The subduction component responsible for melt generation at Fina Nagu does not produce oxidized magmas
- Amphibole and/or serpentine mineral breakdown may be critical for forming oxidized arc magmas

Supporting Information:
- Supporting Information S1
- Figure S1
- Table S1

Correspondence to:
M. N. Brounce,
mbrounce@ucr.edu

Citation:
Brounce, M., K. A. Kelley, R. Stern, F. Martinez, and E. Cottrell (2016), The Fina Nagu volcanic complex: Unusual submarine arc volcanism in the rapidly deforming southern Mariana margin, *Geochem. Geophys. Geosyst.*, *17*, 4078–4091, doi:10.1002/2016GC006457.

Received 25 MAY 2016
Accepted 27 SEP 2016
Accepted article online 29 SEP 2016
Published online 25 OCT 2016

1. Introduction

Arc volcanoes grow large because they reflect long periods of intense eruptive activity at a single location and their lavas are demonstrably influenced by melts and fluids from subducting oceanic plates that move through the mantle on geologically rapid timescales (i.e., faster than plate tectonic timescales) [e.g., *Elliott et al.*, 1997; *Morris et al.*, 1990; *Plank and Langmuir*, 1993; *Turner et al.*, 2001]. These observations indicate that fluids from the subducting slab enter the mantle wedge and cause it to melt [e.g., *Gaetani and Grove*, 2003; *Kelley et al.*, 2010]. Mantle melts, in addition to melts from the subducting slab, form conduit networks and buoyant diapirs in the mantle wedge that transport melts rapidly to the surface [e.g., *Hall and Kincaid*, 2001; *Marsh and Carmichael*, 1974]. This phenomenon broadly describes the mechanisms responsible for producing the volcanic arc in the Marianas, where U-Th, Ra-Th, and U-Pa disequilibria require $<$150,000 years between slab dehydration and eruption of arc magmas [*Avanzinelli et al.*, 2012; *Turner et al.*, 2001].

Anatahan (~16.35°) and Tracey Seamount (~13°40′N, west of Guam) are the southernmost subaerial and submarine stratovolcanoes, respectively, that clearly define the Mariana magmatic arc (Figure 1) [e.g., *Stern et al.*, 2013], despite the continued subduction of the Pacific plate to the south. The proposed extension of arc volcanism further south is the Alphabet seamount volcanic province (~13°00′ to 13°40′N, southwest of Tracey) [*Stern et al.*, 2013], but these seamounts are small in volume and irregularly spaced. Furthermore, Alphabet seamounts have lava compositions with characteristics of both back-arc and arc lavas, which are inconsistent with the model for arc volcano formation described above [*Fryer et al.*, 1998; *Stern et al.*, 2013]. The Fina Nagu volcanic chain extends even further south from the Alphabet seamount volcanic province to

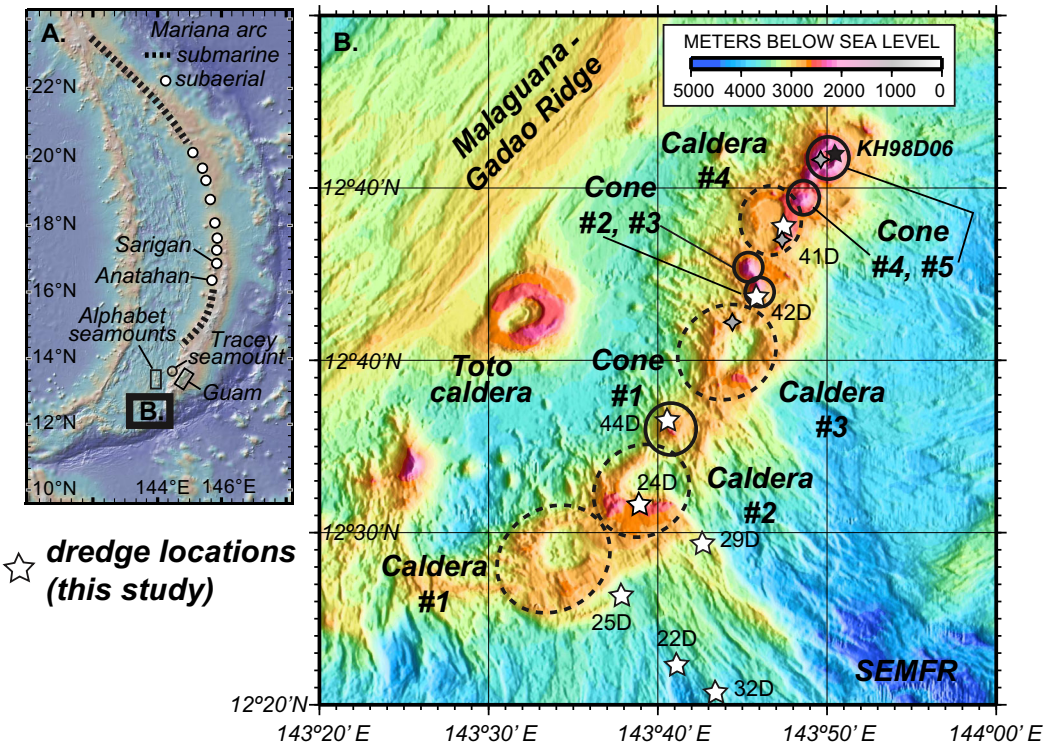

Figure 1. A location map for samples in this study. (a) A map of the Mariana margin, with the location of the submarine arc and subaerial arc marked with a short dashed and white circles, respectively. The black box shows the position of plot b. (b) A bathymetric map showing the Fina Nagu volcanic chain in detail. White, five pointed stars mark the position of dredges that recovered lavas included in this study. Gray, four pointed stars mark the position of ROV *Deep Explorer* dives from expedition EX1605L1 of the *Okeanos Explorer*. Calderas are marked with dashed line circles and cones are marked with solid line circles. Labels such as "22D" mark the dredge number from expedition TN273. The small black star marks the position of sample KH98D06 [*Masuda and Fryer*, 2015]. The basemap for plots a and b was created using GeoMapApp (http://www.geomapapp.org) [*Ryan et al.*, 2009].

~12°20′N, and consists of a ~60 km alignment of four large submarine calderas and five cone-shaped edifices (Figures 1b and 2). Like the arc volcanoes to the north, and unlike the scattered volcanoes of the Alphabet seamounts, those that make up the Fina Nagu volcanic chain align linearly and parallel to the trench and the Malaguana-Gadao Ridge (referred to as the Southern Mariana Trough by *Brounce et al.* [2014]), the southernmost spreading segment of the Mariana Trough.

The Fina Nagu volcanic centers are in some ways unlike traditional arc volcanoes. The caldera features are spaced an average of 12 km apart on the seafloor, compared to 75 km spacing of the subaerial arc. They are located 20–30 km from the back-arc spreading center, which is unusually close compared to central Mariana volcanoes, which are 90–100 km from the back-arc spreading ridge. The Fina Nagu volcanoes are also unusually close to the trench, ~90 km, whereas normal Mariana arc stratovolcanoes are ~220 km west of the trench. Given this unusual location, Fina Nagu volcanoes could represent the southernmost expression of the Mariana volcanic front, or could be related to extension at the Mariana Trough back-arc spreading center—or both. The unusual nature and position of the Fina Nagu volcanic chain provide an opportunity to evaluate the relationship between arc and back-arc basin magmatism, especially to interrogate the relative importance of upper plate stresses versus downgoing plate geometry and dehydration on magma generation.

Here we present major, trace, and volatile element contents and $Fe^{3+}/\sum Fe$ ratios of fresh submarine pillow glasses dredged from four submarine volcanoes of the Fina Nagu volcanic chain, in order to determine whether these reflect arc or back-arc magmatic processes, or some hybrid. We then compare these results with the composition of southeastern Mariana forearc rift (SEMFR, Figure 1) lavas in order to constrain the relationship between melts and fluids from the subducting Pacific plate and volcanism in the southern Mariana convergent margin.

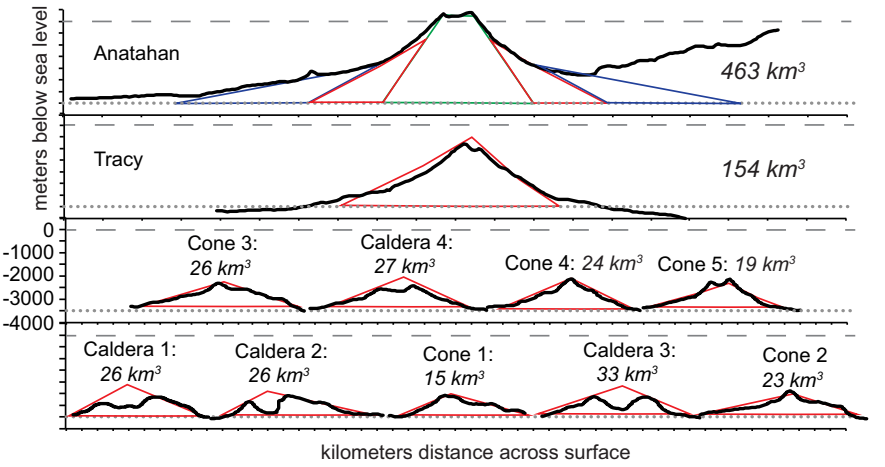

Figure 2. Line profiles taken through the volcanic edifices of the Fina Nagu Volcanic complex, Tracy submarine seamount, and Anatahan volcano, extracted from the basemap of *Ryan et al*. [2009] provided by GeoMapApp (http://www.geomapapp.org). The volumes of volcanic edifices were estimated using two-dimensional bathymetry profiles. Profiles were chosen to transect the center of each volcanic edifice and to extend 3500 m water depth, which is taken as the approximate depth of the base of each edifice. The geometry of each edifice was estimated using simple geometrical shapes, and volume calculations were performed by assuming radial symmetry about the peak height of each volcanic edifice.

2. Geologic Background

The Fina-Nagu volcanic chain consists of four distinct submarine calderas and five volcanic cones in the southernmost Mariana subduction system, southwest of Guam (Figures 1 and 2). It is located between the southern terminus of the Mariana Trough back-arc spreading center, called the Malaguana-Gadao Ridge (referred to as the Southern Mariana Trough by *Brounce et al*. [2014]), and the Southeastern Mariana Forearc Rift, an unusual region of forearc extension and related volcanism [*Fryer*, 1995; *Ribeiro et al*., 2013b]. The southernmost Marianas, between the Malaguana-Gadao Ridge in the west, the Mariana trench in the east and the south, and the Alphabet seamount volcanic province in the north, is a tectonically complex and rapidly deforming region [*Fryer*, 1995; *Kato*, 2003; *Martínez et al*., 2000]. The upper plate is extending southeast-northwest, accommodated by spreading along the Malaguana-Gadao Ridge. In addition, a recent, northeast-southwest extension in the forearc accommodated young volcanic activity ($<$3 Ma) in the Southeastern Mariana Forearc Rift [*Kato*, 2003; *Martínez et al*., 2000; *Ribeiro et al*., 2013a, 2013b]. The Pacific slab is also subducting orthogonally to the Mariana trench in this region at approximately 30 mm/yr [*Bird*, 2003]. The slab progressively deepens from 50 km beneath the forearc rift, to 75–125 km below the Fina Nagu volcanic chain, and to 150–200 km under the Malaguana-Gadao Ridge [*Syracuse and Abers*, 2006].

Lavas erupted in the forearc rift and along the Malaguana-Gadao Ridge are compositionally similar to one another, enriched in incompatible trace elements that are characteristic of input from melts or fluids from the subducting Pacific plate (e.g., Ba, Th; Figures 3–5) [*Brounce et al*., 2014; *Ribeiro et al*., 2013b]. The forearc rift lavas erupted 2.7–3.5 Ma, in a tectonic setting that may have been different from the present configuration due to rapid tectonic reorganization in the southern Marianas since 3 Ma [*Ribeiro et al*., 2013b]. There are no radiometric ages available for Malaguana-Gadao Ridge lavas, but the fresh nature of pillow lavas, including intact glassy rims, the inflated morphology of the ridge, and the presence of a geophysically imaged magma chamber [*Becker et al*., 2010] and active hydrothermal vents [*Yoshikawa et al*., 2012] demonstrates that this is an active spreading center and that the lavas recovered from the axial high are essentially zero age.

Glassy pillow lavas from four volcanoes in the Fina Nagu volcanic chain were dredged from the seafloor between 12°20.3′N and 12°48.0′N during expedition TN273 of the R.V *Thomas G. Thompson* in 2011–2012. Information about sample locations and water depths are provided in supporting information Table 1. Hand sample descriptions can be found in supporting information Table 2. Seafloor observations were made during ROV dives 5, 6, and 7 during Expedition 1605 L1 of NOAA *Okeanos Explorer* in April 2016.

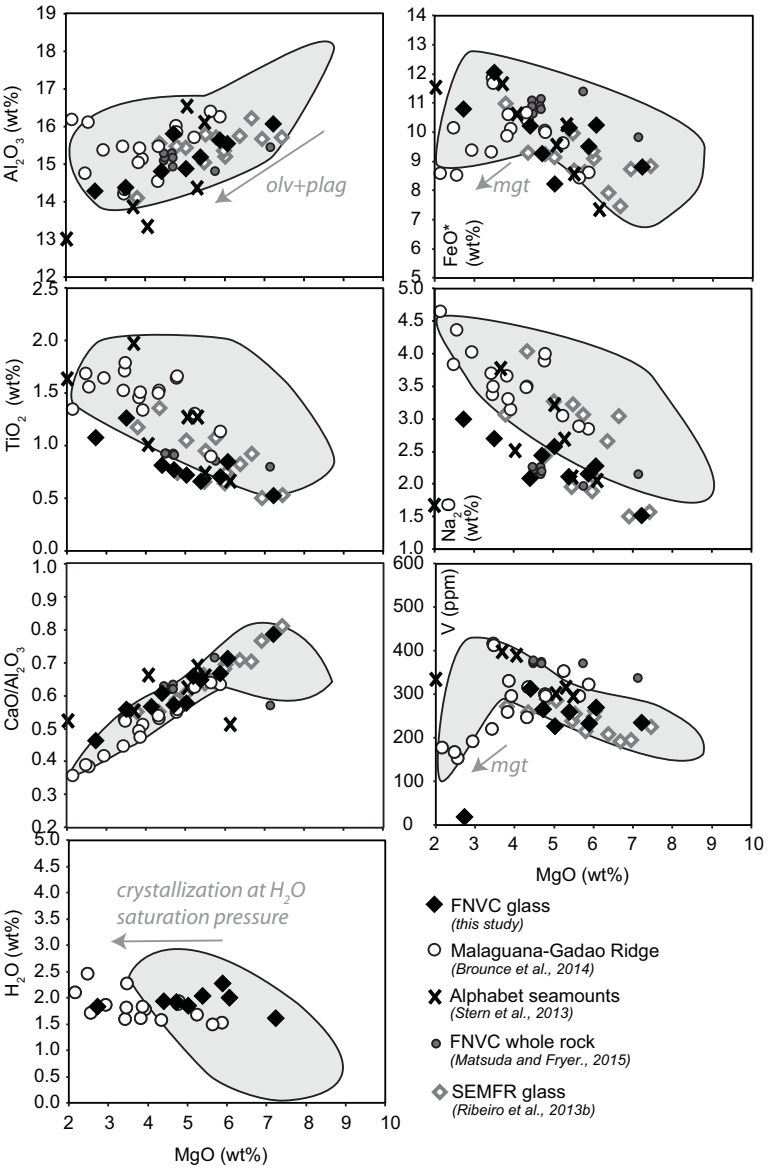

Figure 3. Several plots of major element variations in samples in this study. The gray field shows data from Mariana Trough lavas [*Pearce et al*., 2005; *Stolper and Newman*, 1994]. Arrows in the top two plots show the expected direction that fractional crystallization of (left top plot) olivine and plagioclase and (right top plot, bottom right plot) magnetite will cause glass compositions to go toward. The arrow in the bottom left plot shows the expected direction that combined crystal fractionation and water degassing will move magma compositions toward. Olv, olivine; plag, plagioclase; mgt, magnetite.

3. Analytical Methods

3.1. Major Element and S, Cl Analysis

We analyzed fresh submarine glass chips for major element, S, and Cl contents by electron microprobe at the Smithsonian Institution. During major element analysis, the beam was operated at 10 nA, 15 kV, and a 10 μm beam diameter. Sodium and potassium were measured first with 20 s peak count times to minimize alkali loss. Subsequently, Si, Ti, Al, Fe*, Mn, Ca, and P were measured with 30–40 s peak count times. All data were subject to ZAF correction procedures. Primary calibration standards include VG-2 glass, Kakanui hornblende, anorthite, microcline, ilmentite, and apatite [*Jarosewich et al*., 1980]. The VG-2 and VG-A99 glasses were monitored as secondary standards during each run [*Jarosewich et al*., 1980]. Sulfur and chlorine were measured separately using a beam operated at 80 nA, 15 kV, and 10 μm beam diameter. Scapolite was

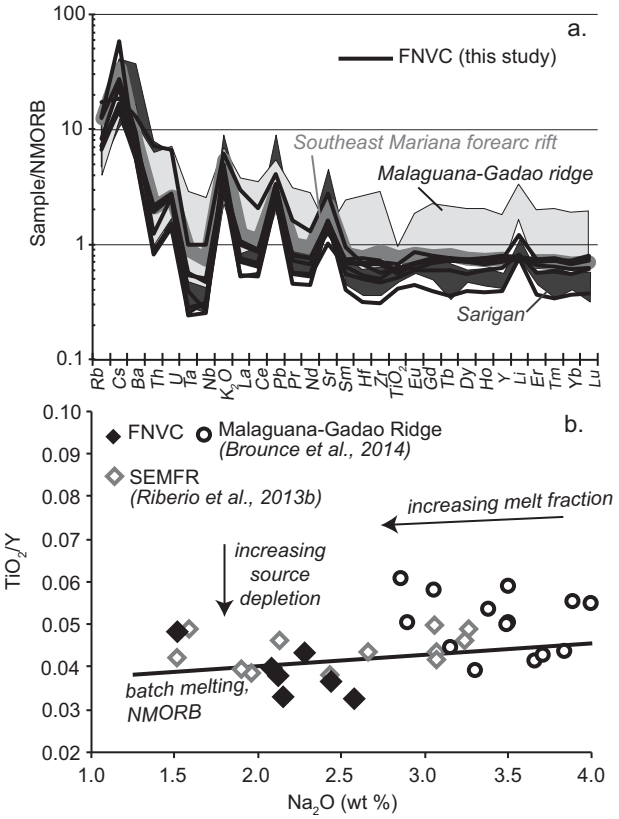

Figure 4. (a) A spider diagram showing the trace element compositions of lavas in this study, normalized to NMORB. The dark gray field shows data from Sarigan volcano [*Brounce et al.*, 2014]. The light gray field shows data from the Malaguana-Gadao Ridge [*Brounce et al.*, 2014]. The thick medium gray line shows the average trace element composition of lavas from the southeastern Mariana forearc rift (SEMFR) [*Ribeiro et al.*, 2013a]. The black lines show trace element compositions of individual lavas from the Fina Nagu volcanic chain [this study]. (b) A plot of TiO_2/Y ratios versus Na_2O contents for Fina Nagu volcanic chain lavas and Malaguana-Gadao ridge lavas. The black line shows the trajectory of a melt produced by bath melting a normal MORB composition mantle from *Kelley et al.* [2006]. Arrows show the general effects of increasing melt fraction and increasing source depletion on the composition of melts.

used as the primary calibration standard (0.529 wt. % S, 1.49 wt. % Cl). The VG-2 (1400 ppm S, 300 ppm Cl) and NIST 620 (1121 ppm S) glasses were used as secondary standards in each run [*Carroll and Rutherford*, 1988; *Jarosewich et al.*, 1980; *Wallace and Carmichael*, 1991]. Further details are provided in supporting information.

3.2. Trace Element Analysis

Abundances of 33 trace elements (Sc, V, Cr, Co, Ni, Cu, Zn, Rb, Sr, Y, Zr, Nb, Cs, Ba, La, Ce, Pr, Nd, Sm, Eu, Gd, Tb, Dy, Er, Tm, Yb, Lu, Hf, Ta, Pb, Th, U) were determined in glass chips by laser-ablation inductively coupled plasma mass spectrometry at the University of Rhode Island on a Thermo X-Series II quadrupole ICP-MS coupled with a New Wave UP 213 Nd-YAG laser-ablation system following techniques outline by *Kelley et al.* [2003] and *Lytle et al.* [2012], normalizing to ^{43}Ca as the internal standard. The laser energy was 0.2–0.3 mJ at the sample surface for a reference spot (60 μm, 10 Hz) on NIST 612 glass and the repeat rate for glasses was reduced to 5 Hz to achieve a slow drilling rate through thin samples. Spot sizes range from 40 to 80 μm. United States Geological Survey glass standards BCR-2g, BHVO-2g, BIR-1g, and Max Planck Institute glass standards GOR-132-G, StHls-G, T1-G, ML3B-G, and KL2-G were used to create linear calibration curves ($R^2 > 0.990$) for each analytical session [*Jochum et al.*, 2006; *Kelley et al.*, 2003]. Samples were analyzed in triplicate and concentrations were reproducible to within 4% rsd for all elements.

3.3. Dissolved H_2O and CO_2

Wafered glass chips were analyzed for dissolved H_2O and CO_2 concentrations by Fourier-transform infrared spectroscopy at the Smithsonian Institution and the University of Rhode Island, on similar instruments and following identical procedures. All samples were analyzed with a Thermo-Nicolet 6700 or a Thermo Nicolet iS50 spectrometer coupled with a Continuum microscope. Spectra were collected between 1000 and 6000 cm^{-1} using a tungsten-halogen source, KBr beamsplitter and a liquid-nitrogen cooled MCT-A detector. The bench, microscope, and samples were continuously purged with air free of water and carbon dioxide using a purge gas generator. Aperture dimensions were selected for each sample depending on the geometry of free glass pathways, ranging in size from 20 × 20 μm to 150 × 150 μm. Dissolved total H_2O concentrations were determined using the 3530 cm^{-1} band. Dissolved CO_3^{2-} concentrations were always below detection at the thickness of glass wafers necessary to generate large pools of glass free from crystals or vesicles, so no data are reported for CO_2 contents of these glasses. Thicknesses of each sample were measured using a piezometric digimatic indicator. Glass densities and absorption coefficients relevant to each absorption band were calculated using methods from *Dixon et al.* [1995] and *Luhr* [2001].

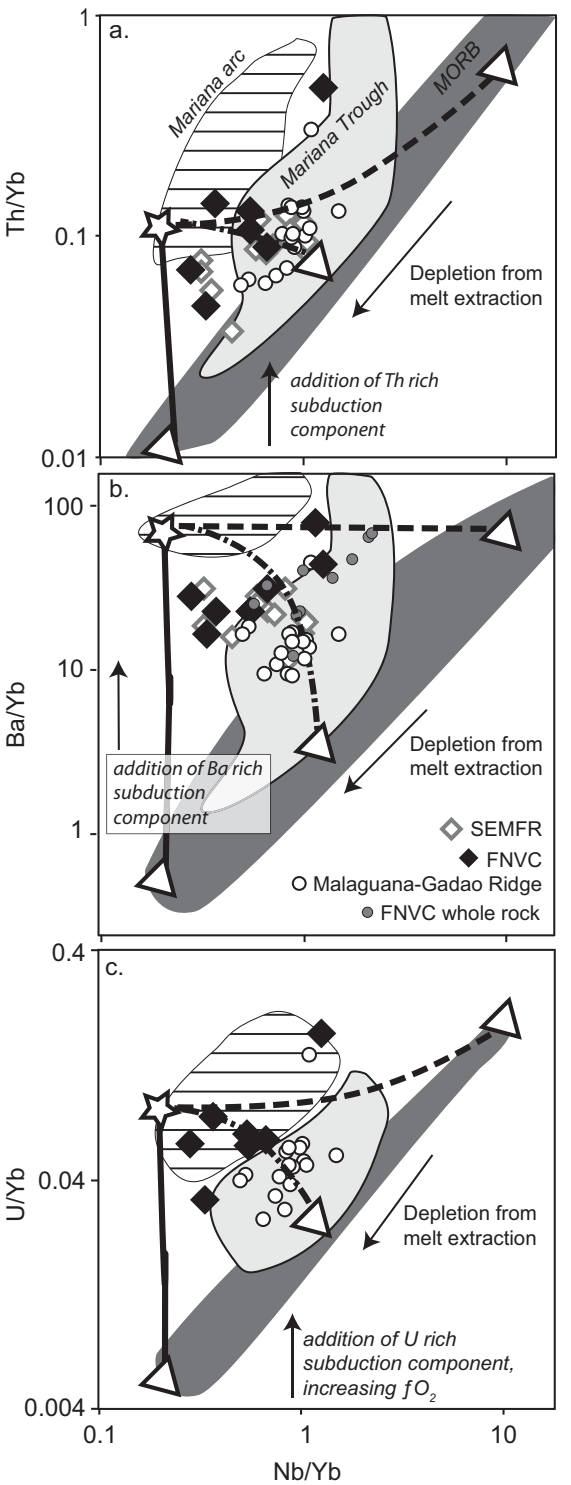

Figure 5. A plot of (a) Th/Yb ratios, (b) Ba/Yb ratios, and (c) U/Yb ratios versus Nb/Yb ratios for samples in this study. The dark gray field shows data for global MORB [*Jenner and O'Neill*, 2012]. The light gray field shows data for the Mariana Trough [*Pearce et al*., 2005; *Stolper and Newman*, 1994]. The white field with horizontal lines shows data for the Mariana arc [*Brounce et al*., 2014]. White circles are data for the Malaguana Gadao ridge [*Brounce et al*., 2014]. White diamonds with gray outlines are data for the SEMFR [*Ribeiro et al*., 2013b]. Small gray circles are bulk pillow glass data for Fina Nagu samples dredged during cruise Hakuho, 1998, and described by *Masuda and Fryer* (2015). The white inverted triangles represent three MORB compositions. The white star represents an average arc composition. The dash, dash-dot, and solid black lines are mixing lines between the MORB compositions and the arc composition.

3.4. Fe^{3+}/Fe Ratios

Wafered glass chips were also analyzed in situ for $Fe^{3+}/\sum Fe$ ratios via micro x-ray absorption near edge structure (μ-XANES) spectroscopy following the methods and techniques of *Cottrell et al*. [2009] at beamline X26A, National Synchrotron Lightsource, Brookhaven National Laboratory. Spectra were collected in fluorescence mode from 7020 to 7220 eV using a 4-element Vortex ME-4 silicon drift diode detector with two single element Vortex-Ex detectors (Hitachi) coupled to an XMap digital spectrometer system, a Si[311] monochromator and a nominal beam size of 9 × 5 μm. A beryllium window was placed over the detector to attenuate high count rates above the main Fe K-alpha fluorescence peak. Reference glass LW_0 was monitored continuously during each experimental session to correct for instrumental drift. Further details related to this correction can be found in *Cottrell et al*. [2009]. Spectra were scrutinized for influence from phenocrysts or microphenocrysts in the glass chips. Details of this procedure can be found in *Brounce et al*. [2014].

4. Composition of Fina Nagu Lavas

The pillow lavas included in this study are aphyric or olivine + plagioclase ± clinopyroxene phyric, variably vesicular basalts. Submarine pillow glasses from the Fina Nagu volcanic chain are basalt to basaltic andesite, with 2.73–7.23 wt. % MgO. The major element and volatile compositions and $Fe^{3+}/\sum Fe$ ratios of these glasses are broadly similar to lavas from the nearby Malaguana-Gadao Ridge and southeast Mariana forearc rift, with the notable exception that Fina Nagu and some southeast Mariana forearc rift glasses have lower TiO_2 and Na_2O concentrations than Malaguana-Gadao Ridge glasses with similar MgO contents (Figures 3 and 4b). Variations in major elements for glasses from Malaguana-Gadao Ridge, the southeast Mariana forearc rift, and Fina Nagu are consistent with olivine + plagioclase ± clinopyroxene fractionation (Figure 3) [*Brounce et al*., 2014]. The glasses have uniform H_2O concentrations (1.9 ± 0.2 wt. %), CO_2 contents below detection, and S concentrations below sulfide saturation (60–353 ppm). The samples were collected in 2358–3800 m water depth, corresponding to confining pressures from the water column of 315–400 bars. The water contents of the glasses indicate that the Fina Nagu magmas degassed water concomitantly with crystal fractionation to maintain a magmatic water concentration that is equal to the confining pressure from the water column at the time of eruption, which is consistent with the depth of lava collection on the seafloor. The low CO_2 contents of these glasses indicate that CO_2 degassing also took place. The low S contents of these glasses could be the result of the loss of sulfur to a vapor phase during degassing, however, the water depths of collection (2358–3800 mbsl) do not permit S degassing (S degassing occurs at water depths <1000 m) [e.g., *Burgisser et al*., 2015]. We emphasize that (1) the H_2O-CO_2 contents are consistent with vapor saturation at the water depths of sample collection (*Newman and Lowenstern*, 2002), (2) the peaks of the reconstructed edifices (i.e., the estimated height above the seafloor of each of the volcanic cones before caldera formation or other mass wasting events) in the Fina Nagu volcanic chain remain in ≥2000 m water depth, and (3) the hand specimens of samples in this study, though moderately vesicular, do not have reticulitic or otherwise volcaniclastic-type textures typical of explosive underwater volcanism. We conclude that the low S contents of the glasses in this study are unlikely to be the result of S degassing, and that the glass chemistries are consistent with degassing of $H_2O + CO_2$ concomitant with crystal fractionation (supporting information Table 1, Figure 3). Fina Nagu submarine glasses are depleted in moderately incompatible trace elements (Figure 4), relative to both normal MORB and Malaguana-Gadao Ridge lavas, but are ~2–70 times enriched over normal MORB in select incompatible trace elements (e.g., Sr, Pb, K_2O, U, Ba, Cs, Rb) [*Elliott et al*., 1997] that are commonly associated with fluids or melts originating from the subducting plate (Figures 4a and 5). Fina Nagu glasses are slightly enriched in LREE and depleted in HREE and high-field strength elements relative to normal MORB compositions (Figure 4a). Fina Nagu submarine glasses have $Fe^{3+}/\sum Fe$ ratios of 0.177–0.223 and $fO_2 \sim$ QFM + 0.7, that are similar across MgO contents, and are slightly oxidized relative to MORB glass, but not as oxidized as modern Mariana arc magmas (Figures 6a and 6d); they are similar to Mariana Trough glasses (including the Malaguana-Gadao Ridge segment). Although we believe S degassing to be an unlikely explanation for the low S contents of Fina Nagu submarine glasses (see above), if S degassing did take place it is possible that the undegassed magmas had higher $Fe^{3+}/\sum Fe$ ratios than those measured in the final erupted glasses. The reducing effects of S degassing have been observed at Agrigan, Erebus, and Kilauea volcanoes [*Kelley and Cottrell*, 2012; *Moussallam et al*., 2014, 2016], and could account for a change in $Fe^{3+}/\sum Fe$ ratios of ~0.05 units (absolute), for a

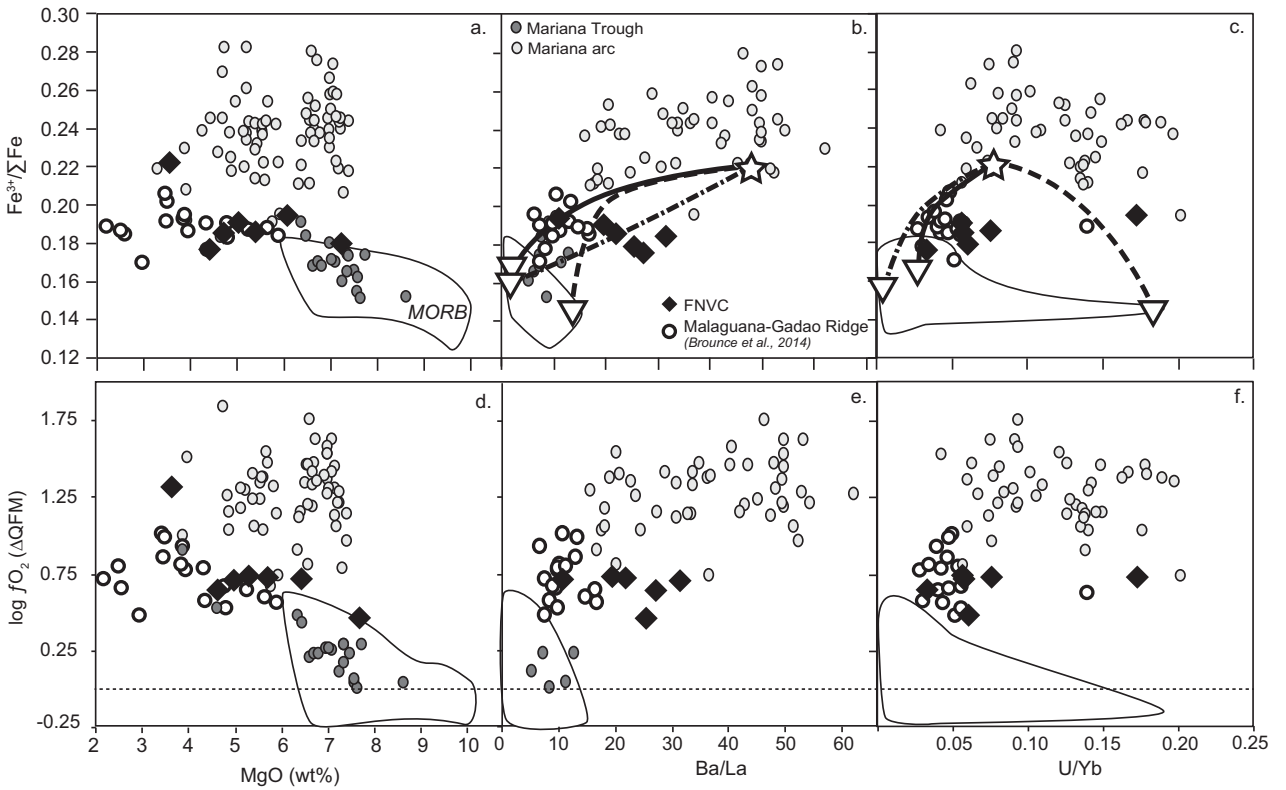

Figure 6. A plot of $Fe^{3+}/\sum Fe$ ratios versus (a) MgO contents and (b) Ba/La ratios, as well as fO_2 (calculated using the algorithm of *Kress and Carmichael* [1991]) relative to the QFM oxygen buffer (according to *Frost* [1991]) at 1200°C versus (c) MgO contents and (d) Ba/La ratios, for samples in this study. Data fields and symbols are as in Figure 5.

magma chemistry similar to that observed at Agrigan volcano [*Kelley and Cottrell*, 2012]. This would mean that the undegassed Fina Nagu magmas have $Fe^{3+}/\sum Fe$ ratios near 0.227–0.273, similar to that observed for the large subaerial and submarine edifices in Mariana arc.

The $Fe^{3+}/\sum Fe$ ratios and fO_2 of Mariana Trough (including the Malaguana-Gadao Ridge segment) and arc basaltic glasses correlate with enrichments in fluid-mobile trace elements (e.g., Ba/La ratio; Figures 6b and 6e), which has been interpreted to arise due to the oxidizing influence of slab fluids in the mantle wedge [*Brounce et al.*, 2014, 2015]. Fina Nagu submarine glasses extend to moderately elevated Ba/La ratios (~30) but only slightly oxidized $Fe^{3+}/\sum Fe$ ratios (0.19) and fO_2 (QFM + 0.7), which do not overlap with the observed trend between oxidation and trace element enrichment for back-arc and arc basaltic glasses in the Marianas. Fina Nagu submarine glasses also have lower TiO_2/V ratios than MORB and Malaguana-Gadao ridge glasses, and overlap entirely with TiO_2/V ratios observed in Mariana arc basaltic glasses (Figure 7).

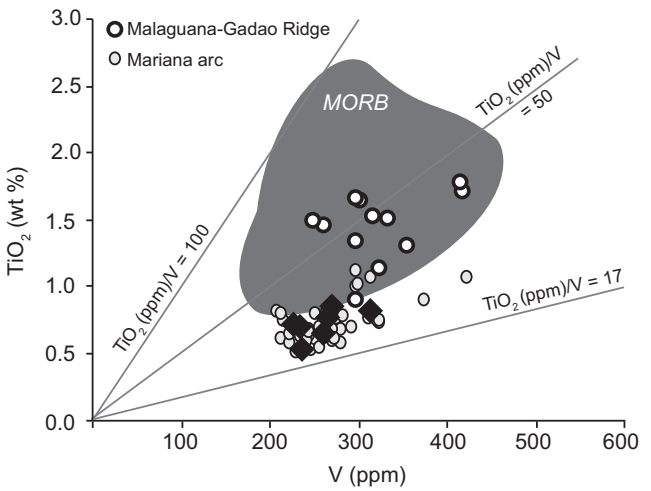

Figure 7. A plot of TiO_2 versus V contents. Symbols are as in Figure 5.

5. Discussion

In the following, we integrate our geochemical data with volume and age estimates for the Fina Nagu

volcanic chain to evaluate the reasons for the unusual distribution of magmatism resulting in many small volcanic edifices at Fina Nagu.

5.1. Geochemical Constraints

The southernmost portion of the Mariana convergent margin is tectonically complex, and asthenospheric mantle flow and pathways for communication between the slab and the surface are likely to be similarly complex [*Ribeiro et al*., 2013a, 2013b; *Stern et al*., 2013]. Malaguana-Gadao Ridge lavas are slightly enriched in heavy rare earth elements and high-field strength elements relative to normal MORB compositions, suggesting that the mantle that flows into the melting triangle beneath the back-arc basin spreading ridge is similar to normal or enriched MORB source mantle [*Brounce et al*., 2014; *Masuda and Fryer*, 2015]. Fina Nagu lavas are more depleted in heavy rare earth and high field strength elements than Malaguana-Gadao Ridge lavas (Figures 4a and 4b), showing similar levels of mantle depletion as the mantle source for subaerial arc volcanoes (e.g., Sarigan volcano, Figure 4a), even when variable extents of melting are taken into consideration (e.g., variable Na_2O contents; Figure 4b). Given the close proximity ($\sim$20–30 km) of the Fina Nagu volcanic chain and the Malaguana-Gadao Ridge, this suggests that mantle undergoes melt extraction at the ridge and the depleted residue flows toward the trench, and is melted again in the source region for Fina Nagu volcanism.

Southeastern Mariana forearc rift lavas are intermediate between Malaguana-Gadao Ridge and Fina Nagu lavas in heavy rare earth and moderately incompatible trace element depletion [*Ribeiro et al*., 2013a, 2013b]. This is an important observation, because it suggests that at the time of eruption of the forearc rift lavas, the twice-depleted residue of melt extraction at the Malaguana-Gadao Ridge and the Fina Nagu volcanic chain did not continue to flow toward the forearc rift to serve as the primary mantle source component for southeastern Mariana forearc rift volcanism. Instead, either the Fina Nagu volcanic chain is younger than the southeastern Mariana forearc rift (i.e., $\ll$ 3 Ma), or, if Fina Nagu volcanism was coincident or older, there must have been a source of mantle flowing into the forearc rift region that was not significantly depleted by prior melt extraction. In the present tectonic configuration, the subducting Pacific plate is $\leq$50 km below the surface of the southeastern Mariana forearc rift [*Syracuse and Abers*, 2006], which may create too small a volume under the forearc rift for significant asthenospheric circulation. However, if there was asthenosphere present below the forearc rift at the time of active volcanism in the rift, the moderately depleted heavy rare earth element compositions of the forearc rift lavas suggest that the mantle had a component of flow that was parallel or subparallel to the trench, in order to bring mantle into the source region of forearc rift lavas that has not previously melted under the Malaguana-Gadao Ridge and the Fina Nagu volcanic chain [*Ribeiro et al*., 2013a].

The trace element and isotopic compositions of global back-arc and arc lavas are commonly influenced by contributions from sediment melts or aqueous fluids from subducting slabs [*Elliott et al*., 1997; *Morris et al*., 1990; *Plank and Langmuir*, 1993]. The compositional signatures of sediment melts (i.e., silicate liquids) and aqueous fluids (i.e., H_2O-rich liquids) are demonstrated in the Marianas by back-arc and arc lavas that are enriched in Ba, U, and sometimes Th relative to moderately incompatible or heavy rare earth elements. Terrigenous sediments that are subducted with the Pacific plate are enriched in thorium that is mobilized into the wedge by sediment melts [*Johnson and Plank*, 2000]. Barium and uranium, on the other hand, partition strongly into aqueous fluids, and are mobilized into the wedge in fluids generated by dehydration of the subducting slab. Uranium in particular is immobile as U^{4+}, but U^{6+} is fluid-mobile, such that U becomes increasingly more mobile in aqueous fluids as fO_2 increases [*Bali et al*., 2011]. Malaguana-Gadao Ridge lavas have variable Nb/Yb ratios that reflect mantle depletion by prior melt extraction. However, Th/Yb, and to a greater extent Ba/Yb and U/Yb ratios in these lavas are elevated relative to MORB and their values indicate that Ba, U, and Th have been added to the mantle source for the Malaguana-Gadao Ridge by both aqueous fluids (in the case of Ba and U) and silicate melts (i.e., melts of the overlying sediment or oceanic crust, in the case of Th) from the subducting Pacific plate (Figures 5a–5c) [e.g., *Pearce et al*., 2005]. The elevated U/Yb ratios indicate that the fO_2 in the zone of melt generation must have been elevated over MORB (Figure 5c). The level of Ba, U, and Th enrichment for Malaguana-Gadao Ridge lavas is similar to that of central and northern Mariana Trough lavas. Fina Nagu lavas show evidence for larger additions of Ba and Th in the mantle source than in the Malaguana-Gadao Ridge mantle source, but not as large as those for the subaerial arc volcanoes (Figures 5a and 5b). Trace element compositions of Malaguana-Gadao Ridge and Fina Nagu lavas are consistent with mixing between variably depleted MORB-like melts (white inverted triangles, Figures

5a–5c) and an arc-like melt (white star, Figures 5a–5c). Although Fina Nagu lavas are not as enriched in Ba, U, or Th as some of subaerial Mariana arc, they are influenced by subduction components to a greater extent than the Malaguana-Gadao ridge.

At a given MgO concentration, the concentrations of TiO_2 and Na_2O can reflect differences in primary melt TiO_2 and Na_2O compositions, which are generated by variable degrees of mantle melting. The Na_2O and TiO_2 concentrations of Fina Nagu lavas are lower than those of the Malaguana-Gadao ridge, and are on the low end of the range of arc lavas at MgO = 6.0 wt. % (at MgO = 6.0 wt. %, TiO_2 ~0.8 wt. % for Fina Nagu, ~1.0 wt. % for Malaguana-Gadao ridge, ~0.6–2.0 wt. % for Mariana arc; Figures 3 and 4b) [*Kelley et al*., 2010]. This suggests that, if the mantle source composition is similar beneath the central arc and Fina Nagu, the mantle under the Fina Nagu volcanic chain produces extents of melting similar to or higher than the mantle under central Mariana arc volcanoes. This is surprising, given the much smaller size of Fina Nagu edifices.

Mariana back-arc basin and arc basaltic glasses are more oxidized than mid-ocean ridge basaltic glasses (Figures 6a–6f) [e.g., *Brounce et al*., 2014]. There is a simple relationship between trace element enrichment (e.g., Ba/La ratios) and oxidation in Mariana backarc basin and arc glasses, suggesting that aqueous slab fluids are oxidized and generate variably oxidized mantle melts, dependent on the ratio of fluid to mantle involved in melt generation (Figures 6b and 6e) [*Brounce et al*., 2014, 2015; *Kelley and Cottrell*, 2012]. This is true of the $Fe^{3+}/\sum Fe$ ratios and also of the calculated magmatic fO_2 values, the latter of which takes into consideration the effects of pressure, temperature, and anhydrous major element chemistry on the relationship between the oxidation state of Fe of fO_2 (Figure 6e). Surprisingly, Fina Nagu glasses do not follow the relationship between increasing Ba/La and $Fe^{3+}/\sum Fe$ ratios that is defined by >150 submarine glass chips and olivine hosted melt inclusions from Mariana arc volcanoes, the Mariana Trough, and global MORB, including submarine glass chips that record the initiation of subduction along the Izu-Bonin-Mariana convergent margin (Figures 6b and 6e) [*Brounce et al*., 2014, 2015; *Cottrell and Kelley*, 2011; *Kelley and Cottrell*, 2009].

Volcanic degassing has been shown to have an effect on the $Fe^{3+}/\sum Fe$ ratios and fO_2 of olivine-hosted basaltic melt inclusions from Erebus, Agrigan, and Kilauea volcanoes [*Kelley and Cottrell*, 2012; *Moussallam et al*., 2014, 2016]. In these cases, volcanic degassing led to a decrease in $Fe^{3+}/\sum Fe$ ratios, and this was tied specifically to S degassing at magmatic temperatures. If S degassing has not occurred from the Fina Nagu magmas before eruption on the seafloor (see above), then no significant shift in $Fe^{3+}/\sum Fe$ ratios is expected. It has also been proposed that degassing and preferential loss of (1) H_2 [e.g., *Holloway*, 2004], or (2) CO [*Mathez and Delaney*, 1981] can oxidize magmas, but two lines of evidence demonstrate that the effect is small. First, basaltic melt inclusions and submarine glasses from the Mariana arc that span >4 wt. % H_2O and >1000 ppm CO_2 do not demonstrate any significant variations in $Fe^{3+}/\sum Fe$ ratios or fO_2 that indicate that H_2O-CO_2 degassing impacts the redox state of their degassing melts significantly [*Brounce et al*., 2014]. Second, observations of natural andesitic to rhyolitic eruptive products demonstrate that the loss of several weight percent of water does not change the measured $Fe^{3+}/\sum Fe$ ratios or inferred fO_2 of the associated magmas studied [*Crabtree and Lange*, 2012; *Waters and Lange*, 2016].

In the absence of degassing, the redox state of Fina Nagu lavas may reflect a mantle source or melt generation process. The elevated U/Yb ratios (Figure 5c) and lower TiO_2/V ratios (Figure 7) of Fina Nagu lavas are consistent with measured $Fe^{3+}/\sum Fe$ ratios and calculated magmatic fO_2 values that are elevated over MORB, and though TiO_2/V ratios overlap with arc samples, slightly lower U/Yb ratios in Fina Nagu lavas indicate that fO_2 may not have been as high as for the most oxidized arc samples (Figures 5c, 6c, and 6f). Further, it appears as though mixing between variably depleted MORB-like melts (inverted triangles, Figures 6b and 6c) and an arc-like melt (white star, Figures 6b and 6c) cannot explain the lack of relationship between trace element enrichment and oxidation observed in Fina Nagu lavas, suggesting that the subduction component responsible for oxidation along the Mariana arc is different or not present in the zone of melt generation for Fina Nagu lavas. This is similar to observations of the Valu Fa ridge, where there is evidence for a subduction component in trace element compositions, but no obvious relationship between the subduction component and the oxidation state of the lavas [*Jenner et al*., 2015].

The subducting Pacific plate is between 75 and 125 km depth (2.5–4 GPa) below the Fina Nagu volcanic chain, which is shallower than the average depth to the slab under subaerial Mariana arc volcanoes (150–

175 km, 5–5.8 GPa) [*Syracuse and Abers*, 2006]. The relatively shallow depths of the subducting slab under Fina Nagu correspond to sediment surface temperatures of ~380–800°C, which are sufficiently high to dehydrate and melt the sediment column [*Van Keken et al*., 2011]. The upper 1.5 km of oceanic crust between 75 and 125 km has temperatures of 275–800°C, where hydrous minerals such as amphibole and lawsonite are stable, though the high end of the range ($T > 600$°C) should cause lawsonite breakdown [*Van Keken et al*., 2011]. The slab's lower crust and mantle rocks remain cool enough that hydrous mineral phases such as lawsonite, chlorite, amphibole (lower crust), and serpentine, chlorite (mantle) remain stable [*Van Keken et al*., 2011]. The greater depths of the subducting slab under subaerial Mariana arc volcanoes lead to amphibole breakdown in the upper 1.5 km of the oceanic crust and chlorite/serpentine breakdown in the subducting lithosphere [*Van Keken et al*., 2011]. The lack of correlation between Ba/La and $Fe^{3+}/\sum Fe$ ratios in Fina Nagu glasses may indicate therefore that deserpentinization and/or amphibole breakdown reactions in the subducting slab are important in generating fluids that are capable of oxidizing the melts produced in the mantle wedge. Serpentinization reactions on the seafloor transform olivine to magnetite, releasing H_2-rich fluids and leaving the oceanic lithosphere with a more oxidized magnetite-bearing assemblage. If high pressure, high temperature deserpentinization reactions transform magnetite back to olivine, the fluids produced from that reaction must contain oxidized components (e.g., SO_x species) [*Debret et al*., 2016]. Similarly, amphibole can contain Fe^{3+} and the breakdown reactions that produce H_2O-rich fluids that would equilibrate with that oxidizing assemblage. The breakdown of an oxidizing assemblage could potentially oxidized slab components to fluid-mobile agents of oxidation (e.g., S^{2-} to SO_3) [*Gaillard et al*., 2015]. The fluid that contributes to Fina Nagu volcanism, unlike the rest of the arc, may have oxygen fugacity similar to the ambient upper mantle (i.e., near the quartz-fayalite-magnetite oxygen buffer) [*Cottrell and Kelley*, 2011], or may not have significant concentrations of species capable of producing oxidized mantle melts (e.g., S, Fe) [*Mungall*, 2002]. That magmatic fO_2 remained relatively low from mantle melting through to eruption is supported by the lack of magnetite fractionation from melts with higher than ~3–4 wt. % MgO (as monitored by V contents, Figure 3), despite all samples having dissolved H_2O contents elevated over typical MORB [e.g., *Osborn*, 1959; *Sisson and Grove*, 1993; *Saal et al*., 2002].

5.2. Volume and Age Estimates

Despite inferences from geochemical observations that the extents of melting required to generate the composition of Fina Nagu lavas are similar to or greater than those responsible for forming arc lavas, the volume of individual volcanic edifices in the Fina Nagu volcanic chain are remarkably small ~24 km^3. This is an order of magnitude smaller than nearby Mariana arc volcano Tracy seamount or Anatahan (Figure 2). Although the Fina Nagu samples lack radiometric age constraints, the Fina Nagu volcanoes appear to become younger from SW to NE along the chain. Several lines of evidence support this conclusion: seafloor fabrics, the appearance of mud and manganese coated lavas, pillow lava appearance on the seafloor, and hydrothermal activity.

Although interpretations based solely on seafloor fabrics can be tenuous, morphologically more mature, and possibly older volcanic centers in the southwest appear as calderas with relatively shallowly sloping caldera walls that may have eroded and degraded over time (Caldera #1, Figure 1). The calderas in the northeast have steeper caldera walls that may reflect more recent volcanism (Caldera #4, Figure 1), along with the presence of intact volcanic cones in the northeast (Cones #4, #5, Figure 1). An apparent age progression in Fina Nagu volcanism is broadly supported by recent observations of the seafloor during EX1605 of the NOAA ship *Okeanos Explorer* and ROV *Deep Discoverer* (locations marked with gray, four pointed stars, Figure 1). Video imagery of exposures on the north wall of Caldera #3 shows angular to subangular talus and occasional pillow flow or dike outcrop with light to moderate sediment cover (Figure 8a). Caldera #3 appears to have undergone episodes of mass wasting since the most recent lava flow, revealing dike outcrops on the caldera wall and fragmented pillow flows to produce talus fields. This suggests some time has passed since the most recent lava flow in the region explored by *Deep Discoverer*. Video imagery of the east wall of Caldera #4 reveals abundant and intact pillow lobes and sheet flows with light sediment cover, suggesting that these undisturbed flows happened recently enough to preserve their original emplacement on the seafloor (Figure 8b). Video imagery of two resurgent dome structures in the crater floor of Cone #5 reveals extinct but intact, large, hydrothermal chimney structures (Figure 8c), and low temperature, active fluid seeping with associated remnant worm tubes (Figure 8d). The coherence and apparently emplaced nature of these relatively delicate structures (e.g., worm tubes, flange, and chimney structures) suggests

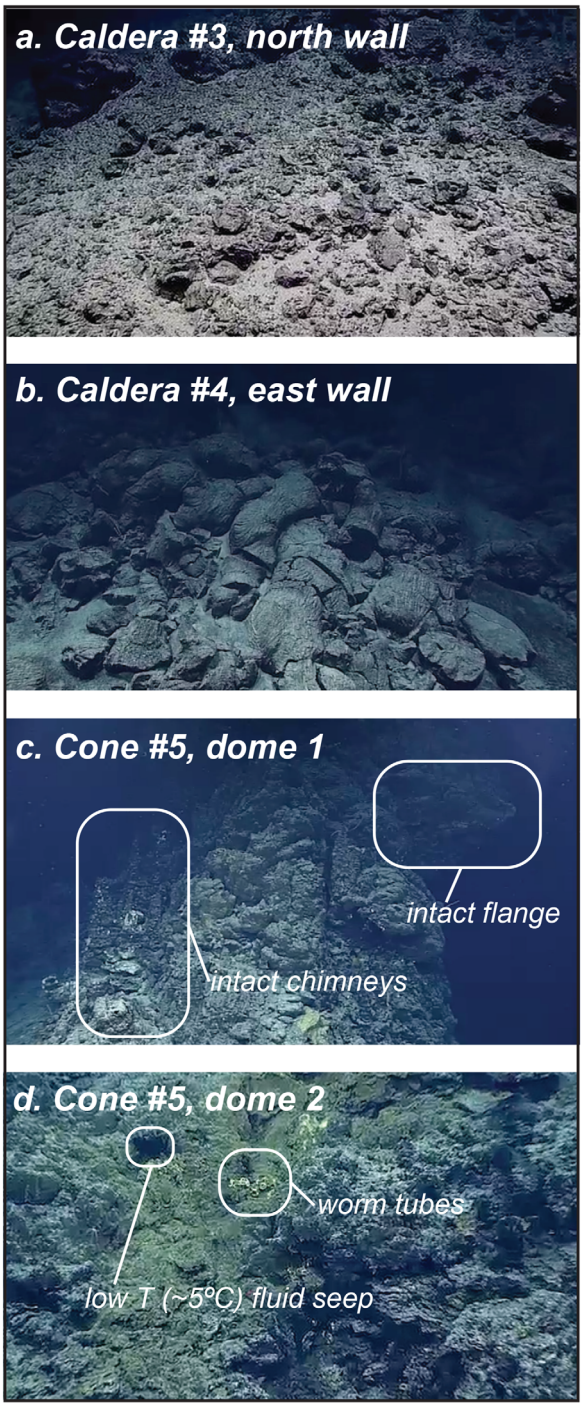

Figure 8. Still images from video feed captured by ROV *Deep Explorer* during expedition EX1605L1. Video credit to NOAA OER, NOAA vessel *Okeanos Explorer*.

that Cone #5 was active until very recently, or at least more recently than Caldera #3 and Caldera #4. The sum of bathymetric, dredge sample, and ROV seafloor images supports the hypothesis that Fina Nagu volcanoes are older in the SW and younger in the NE.

5.3. Fina Nagu Volcanic Chain: An Arc Volcano, Distributed?

The estimated cumulative volume of the Fina Nagu volcanic chain is approximately 217 km^3, which is slightly larger than Tracy seamount (~154 km^3) and roughly half the size of Anatahan volcano (~463 km^3; Figure 2). In conjuction with information that the region is actively extending, this suggests that while the main aspects of melt generation under the Fina Nagu volcanic chain are similar to Mariana arc volcanoes, the melts were distributed along the volcanic chain rather than being focused in a single volcanic edifice. If the melts produced under the volcanic chain were focused into a single volcano, the edifice would be approximately the size of Tracy seamount. It is likely that complex lithospheric deformation patterns, generated by perpendicular spreading directions at the Malaguana-Gadao ridge and the southeastern Mariana forearc rift, are controlling melt transport through the lithosphere to a magnitude not seen elsewhere along the Mariana volcanic arc. This deformation encourages the formation of ridge-like, or volcanic chain features, and explains both the small volume of Fina Nagu volcanic structures and their close spacing on the seafloor.

It is possible that melt focusing in the crust [e.g., *Stern et al.*, 2013] may have progressed toward the northeast through time. The Fina Nagu volcanic chain is aligned in the direction of rifting in the southeastern Mariana forearc rift, and this generates stretching or rifting of the overriding plate lithosphere [e.g., *Martinez et al.*, 2014] relative to diapir-like sources of arc melts tied to the subducting Pacific plate, which generated the chain of volcanoes. Alternatively, the diapir-like sources of arc melts may themselves migrate relative to the subducting slab, and therefore also relative to the overriding plate (i.e., the path of diapirs through the wedge could migrate trench-parallel toward the northeast), and this could generate the observed morphology of the Fina Nagu volcanoes on the overriding plate. A change in the path of diapirs in the wedge could arise due to a change in shape of the subducting Pacific plate in this region, producing a change in the conditions of fluid or melt transfer from the slab surface and through the mantle wedge. It is also possible that a combination of both processes is responsible for the formation of the Fina Nagu volcanic chain.

6. Conclusions

The results presented here suggest that, prior to infiltration of sediment melts and aqueous slab fluids, Fina Nagu lavas were produced from a depleted mantle that is broadly similar in composition to the depleted mantle that is the source for subaerial arc volcanism in the Marianas. Fina Nagu lavas are intermediate between Malaguana-Gadao Ridge lavas and subaerial Mariana arc lavas in trace element ratios that track the input of aqueous slab fluids to the mantle wedge. The lack of relationship between increasing Ba/La ratios and oxidation suggests that this arises because the aqueous fluid percolating through the mantle source is different in composition than elsewhere in the Marianas. The TiO_2 contents of Fina Nagu lavas indicate melt fractions similar to those produced at Mariana arc volcanoes, that, when combined with volume estimates for the Fina Nagu volcanic edifices, suggest melt generation in the mantle wedge takes place with similar mechanisms to arc melt generation, and that the small size of Fina Nagu volcanic edifices arises due to the distribution of these melts among many edifices on the seafloor. A possible progression of volcanism from the southwest to the northeast through time may be generated as the result of lithospheric extension in the southeastern Mariana forearc rift, or a change in the path of melt diapirs through the wedge, or both, generating the unusual chain of small volume, submarine arc volcanic features in the southern Mariana convergent margin.

Acknowledgments

We would like to thank Frances Jenner and two anonymous reviewers for their careful attention to our paper. We would like to thank the captain and crew aboard the *Thomas G. Thompson* during expedition TN273, and aboard the NOAA vessel *Okeanos Explorer* and ROV *Deep Discoverer* during expedition EX1605L1. We thank M. Lytle, B. Covellone, J. Ribeiro, W. Lieu, and E. Jordan for leadership and assistance during dredging operations for TN273. We thank A. Lanzirotti, W. Rao, and S. Wirick for assistance in beamline operations at NSLS BNL. Access to NSLS BNL was supported by the US Department of Energy under contract DE-AC02-98CH10886. We acknowledge support from NSF grant OCE-0961811 to Martinez, NSF OCE-0961559 and NSF EAR-1258940 to Kelley, NSF EAR-0841006 to Cottrell, and NSF OCE-0961352 to Stern. NSF OCE-1258771 provides curatorial support for marine geological samples at the University of Rhode Island. Supporting data are included as data tables in a supporting information file. Additional information may be obtained from the first author at mbrounce@ucr.edu.

References

Avanzinelli, R., J. Prytulak, S. Skora, A. Heumann, G. Koetsier, and T. Elliott (2012), Combined ^{238}U-^{230}Th and ^{235}U-^{231}Pa constraints on the transport of slab-derived material beneath the Mariana Islands, *Geochim. Cosmochim. Acta*, *92*, 308–328.

Bali, E., A. Audetat, and H. Keppler (2011), The mobility of U and Th in subduction zone fluids: an indicator of oxygen fugacity and fluid salinity, *Contri. Mineralogy Petr.*, *161*, 597–613.

Becker, N.C., P. Fryer, and G. F. Moore (2010), Malaguana-Gadao Ridge: Identification and implications of a magma chamber reflector in the southern Mariana Trough, *Geochem. Geophys. Geosyst.*, *11*, Q04X13, doi:10.1029/2009GC002719.

Bird, P. (2003), An updated digital model of plate boundaries, *Geochem. Geophys. Geosyst.*, *4*(3), 1027, doi:10.1029/2001GC000252.

Brounce, M., K. A. Kelley, and E. Cottrell (2014), $Fe^{3+}/\sum Fe$ variations in Mariana Arc basalts and primary fO_2 of the mantle wedge, *J. Petrol.*, *55*, 2513–2536.

Brounce, M., K. A. Kelley, E. Cottrell, and M. K. Reagan (2015), Temporal evolution of mantle wedge oxygen fugacity during subduction initiation, *Geology*, *43*, 775–778.

Burgisser, A., M. Alletti, and B. Scaillet (2015), Simulating the behavior of volatiles belonging to the C-O-H-S system in silicate melts under magmatic conditions with the software D-Compress, *Comput. Geosci.*, *79*, 1–14.

Carroll, M. R., and M. J. Rutherford (1988), Sulfur speciation in hydrous experimental glasses by varying oxidation state: Results from measured wavelength shifts of sulfur X-rays, *Am. Mineral.*, *73*, 845–849.

Cottrell, E., and K. A. Kelley (2011), The oxidation state of Fe in MORB glasses and the oxygen fugacity of the upper mantle, *Earth Planet. Sci. Lett.*, *305*(3–4), 270–282.

Cottrell, E., K. A. Kelley, A. Lanzirotti, and R. A. Fischer (2009), High-precision determination of iron oxidation state in silicate glasses using XANES, *Chem. Geol.*, *268*(3–4), 167–179.

Crabtree, S., and R. Lange (2012), An evaluation of the effect of degassing on the oxidation state of hydrous andesite and dacite magmas: A comparison of pre- and post-eruptive Fe^{2+} concentrations, *Contrib. Mineral. Petrol.*, *163*, 209–224.

Debret, B., M.-A., Millet, M.-L. Pons, P. Bouihol, E. Inglis, and H. Wiliams (2016), Isotopic evidence for iron mobility during subduction, *Geology*, *44*, 215–218.

Dixon, J. E., E. M. Stolper, and J. R. Holloway (1995), An experimental study of water and carbon dioxide solubilities in mid-ocean ridge basaltic liquids. Part I. Calibration and solubility models, *J. Petrol.*, *36*(6), 1607–1630.

Elliott, T., T. Plank, A. Zindler, W. White, and B. Bourdon (1997), Element transport from slab to volcanic front at the Mariana arc, *J. Geophys. Res.*, *102*(B7), 14,991–15,019.

Frost, B. R. (1991), Introduction to oxygen fugacity and its petrologic importance, *Rev. Mineral. Geochem.*, *25*, 1–9.

Fryer, P. (1995), Geology of the Mariana Trough, in *Backarc Basins: Tectonics and Magmatism*, edited by B. Taylor, pp. 237–279, Plenum, N. Y.

Fryer, P., H. Fujimoto, M. Sekine, L. E. Johnson, J. Kasahara, H. Masuda, T. Gamo, T. Ishii, M. Ariyoshi, and K. Fujioka (1998), Volcanoes of the southwestern extension of the active Mariana island arc: New swatch-mapping and geochemical studies, *Island Arc*, *7*, 596–607.

Gaetani, G. A., and T. L. Grove (2003), Experimental constraints on melt generation in the mantle wedge: Inside the subduction factory, *Geophys. Monogr. AGU*, *138*, 107–134.

Gaillard, F., B. Scaillet, M. Pichavant, and G. Iacono-Marziano (2015), The redox geodynamics linking basalts and their mantle sources through space and time, *Chem. Geol.*, *418*, 217–233.

Hall, P. S., and C. Kincaid (2001), Diapiric flow at subduction zones: A recipe for rapid transport, *Science*, *292*, 2472–2575.

Holloway, J. (2004), Redox reactions in seafloor basalts: Possible insights into silicic hydrothermal systems, *Chem. Geol.*, *210*, 225–230.

Jarosewich, E., J. Nelen, and J. Norberg (1980), Reference samples for electron microprobe analysis, *Geostand. Newsl.*, *4*, 43–47.

Jenner, F. E., and H. O'Neill (2012), Analysis of 60 elements in 616 ocean floor basaltic glasses, *Geochem. Geophys. Geosyst.*, *13*, Q02005, doi:10.1029/2011GC004009.

Jenner, F. E., E. H. Hauri, E. S. Bullock, S. Konig, R. J. Arculus, J. A. Mavrogenes, N. Mikkelson, and C. Goddard (2015), The competing effects of sulfide saturation versus degassing on the behavior of the chalcophile elements during the differentiation of hydrous melts, *Geochem. Geophys. Geosyst.*, *16*, 1490–1507, doi:10.1002/2014GC005670.

Jochum, K. P., et al. (2006), The preparation and preliminary characterisation of eight geological MPI-DING reference glasses for in-situ microanalysis, *Geostand. Geoanal. Res.*, *24*(1), 97–133.

Johnson, M. C., and T. Plank (2000), Dehydration and melting experiments constrain the fate of subducted sediments, *Geochem. Geophys. Geosyst.*, *1*(12), 1007, doi:10.1029/1999GC000014.
Kato, T. (2003), Geodetic evidence of back-arc spreading in the Mariana Trough, *Geophys. Res. Lett.*, *30*(12), 1625, doi:10.1029/2002GL016757.
Kelley, K. A., and E. Cottrell (2009), Water and the oxidation state of subduction zone magmas, *Science*, *325*(5940), 605–607.
Kelley, K., T. Plank, J. Ludden, and H. Staudigel (2003), Composition of altered oceanic crust at ODP Sites 801 and 1149, *Geochem. Geophys. Geosyst.*, *4*(6), 8910, doi:10.1029/2002GC000435.
Kelley, K. A., T. Plank, T. L. Grove, E. M. Stolper, S. Newman, and E. Hauri (2006), Mantle melting as a function of water content beneath back-arc basins, *J. Geophys. Res.*, *111*, B09208, doi:10.1029/2005JB003732.
Kelley, K. A., T. Plank, S. Newman, E. M. Stolper, T. L. Grove, S. Parman, and E. Hauri (2010), Mantle melting as a function of water content beneath the Mariana arc, *J. Petrol.*, *51*, 1711–1739.
Kelley, K. A., and E. Cottrell (2012), The influence of magmatic differentiation on the oxidation state of Fe in a basaltic arc magma, *Earth Planet. Sci. Lett.*, *329–330*, 109–121.
Kress, V. C., and I. S. E. Carmichael (1991), The compressibility of silicate liquids containing Fe_2O_3 and the effect of composition, temperature, oxygen fugacity and pressure on their redox states, *Contri. Mineralogy Petr.*, *108*, 82–92.
Luhr, J. F. (2001), Glass inclusions and melt volatile contents at Paricutin Volcano, Mexico, *Contrib. Mineral. Petrol.*, *142*(23), 261–283.
Lytle, M. L., K. A. Kelley, E. H. Hauri, J. B. Gill, D. Papia, and R. J. Arculus (2012), Tracing mantle sources and Samoan influence in the northwestern Lau back-arc basin, *Geochem. Geophys. Geosyst.*, *13*, Q10019, doi:10.1029/2012GC004233.
Marsh, B. D., and I. S. E. Carmichael (1974), Benioff zone magmatism, *J. Geophys. Res.*, *79*(8), 1196–1206.
Martínez, F., P. Fryer, and N. Becker (2000), Geophysical characteristics of the southern Mariana Trough, 11°50′N–13°40′N, *J. Geophys. Res.*, *105*(B7), 16,591.
Martinez, F., P. Fryer, J. Sleeper, and R. Stern (2014), Hydrous lithosphere and diffuse crustal accretion and tectonics in the southern Mariana margin: A possible analog for subduction zone infancy and ophiolites, Abstract T52B-03 presented at 2014 Fall Meeting, AGU, San Francisco, Calif., 15–19 Dec.
Masuda, H., and P. Fryer (2015), Geochemical characteristics of active backarc basin volcanism at the southern end of the Mariana Trough, in *Subseafloor Biosphere Linked to Hydrothermal Systems: TAIGA Concept*, edited by J.-i. Ishibashi, K. Okino, and M. Sunamura, pp. 261–273, Springer, Japan.
Mathez, E. A., and J. R. Delaney (1981), The nature and distribution of carbon in submarine basalts and peridotite nodules, *Earth Planet. Sci. Lett.*, *56*, 217–232.
Morris, J. D., W. P. Leeman, and F. Tera (1990), The subducted component in island arc lavas: Constraints from Be isotopes and B-Be systematics, *Nature*, *344*(6261), 31–36.
Moussallam, Y., C. Oppenheimer, B. Scaillet, F. Gaillard, P. Kyle, N. Peters, M. Hartley, K. Berlo, and A. Donovan (2014), Tracking the changing oxidation state of Erebus magmas, from mantle to surface, driven by magma ascent and degassing, *Earth Planet. Sci. Lett.*, *393*, 200–209.
Moussallam, Y., M. Edmonds, B. Scaillet, N. Peters, E. Gennaro, I. Sides, and C. Oppenheimer (2016), The impact of degassing on the oxidation state of basaltic magmas: A case study of Kilauea volcano, *Earth Planet. Sci. Lett.*, *450*, 317–325.
Mungall, J. (2002), Roasting the mantle: Slab melting and the genesis of major Au and Au-rich Cu deposits, *Geology*, *30*, 915–918.
Newman, S., and J. B. Lowenstern (2002), VolatileCalc: A silicate melt-H_2O-CO_2 solution model written in Visual Basic for excel, *Comput. Geosci.*, *28*, 597–604.
Osborn, E. F. (1959), Role of oxygen pressure in the crystallization and differentiation of basaltic magma, *Am. J. Sci.*, *257*, 609–647.
Pearce, J. A., R. J. Stern, S. H. Bloomer, and P. Fryer (2005), Geochemical mapping of the Mariana arc-basin system: Implications for the nature and distribution of subduction components, *Geochem. Geophys. Geosyst.*, *6*, Q07006, doi:10.1029/2004GC000895.
Plank, T., and C. H. Langmuir (1993), Tracing trace elements from sediment input to volcanic output at subduction zones, *Nature*, *362*, 739–742.
Ribeiro, J. M., R. J. Stern, K. A. Kelley, F. Martinez, O. Ishizuka, W. I. Manton, and Y. Ohara (2013a), Nature and distribution of slab-derived fluids and mantle sources beneath the Southeast Mariana forearc rift, *Geochem. Geophys. Geosyst.*, *14*, 4585–4607, doi:10.1002/ggge.20244.
Ribeiro, J. M., et al. (2013b), Geodynamic evolution of a forearc rift in the southernmost Mariana Arc, *Island Arc*, *22*(4), 453–476.
Ryan, W. B. F., et al.(2009), Global multi-resolution topography synthesis, *Geochem. Geophys. Geosyst.*, *10*, Q03014, doi:10.1029/2008GC002332.
Saal, A. E., E. H. Hauri, C. H. Langmuir, and M. R. Perfit (2002), Vapour undersautration in primitive mid-ocean-ridge basalt and the volatile content of Earth's upper mantle, *Nature*, *419*, 451–455.
Sisson, T. W., and T. L. Grove (1993), Experimental investigations of the role of H_2O in calc-alkaline differentiation and subduction zone magmatism, *Contrib. Mineral. Petrol.*, *113*, 143–166.
Stern, R. J., Y. Tamura, H. Masuda, P. Fryer, F. Martinez, O. Ishizuka, and S. H. Bloomer (2013), How the Mariana Volcanic Arc ends in the south, *Island Arc*, *22*(1), 133–148.
Stolper, E., and S. Newman(1994), The role of water in the petrogenesis of Mariana Trough magmas, *Earth Planet. Sci. Lett.*, *121*, 293–325.
Syracuse, E. M., and G. A. Abers (2006), Global compilation of variations in slab depth beneath arc volcanoes and implications, *Geochem. Geophys. Geosyst.*, *7*, Q05017, doi:10.1029/2005GC001045.
Turner, S., P. Evans, and C. J. Hawkesworth (2001), Ultrafast source-to-surface movement of melt at Island Arcs from 226Ra-230Th systematics, *Science*, *292*, 1363–1366.
Van Keken, P. E., B. R. Hacker, E. M. Syracuse, and G. A. Abers (2011), Subduction factory: 4. Depth-dependent flux of H_2O from subducting slabs worldwide, *J. Geophys. Res.*, *116*, B01401, doi:10.1029/2010JB007922.
Wallace, P. J., and I. S. E. Carmichael (1991), Sulfur in basaltic magmas, *Geochim. Cosmochim. Acta*, *56*, 1863–1874.
Waters, L. E., and R. Lange (2016), No effect of H_2O degassing on the oxidation state of magmatic liquids, *Earth Planet. Sci. Lett.*, *447*, 48–59.
Yoshikawa, S., K. Okino, and M. Asada (2012), Geomorphological variations at hydrothermal sites in the southern Mariana Trough: Relationship between hydrothermal activity and topographic characteristics, *Mar. Geol.*, *303–306*, 172–182.